



# Simulation model for energy consumption and acoustic underwater communication of autonomous underwater vehicles

Peter Danielis<sup>1</sup> · Helge Parzyjegl<sup>1</sup> · Mostafa Assem Mohamed Ali<sup>1</sup> · Frank Sill Torres<sup>2</sup>

Received: 20 October 2021 / Accepted: 26 October 2021 / Published online: 29 November 2021  
© The Author(s) 2021

## Abstract

Recently, cooperative autonomous underwater vehicles (AUVs) have been deployed in application areas such as surveillance and protection of maritime infrastructures for inspection and monitoring purposes. These cooperative methodologies require wireless transmission of data between the different AUVs operating in the underwater environment. Communication over ranges exceeding 100 m exclusively relies on underwater acoustic communication. However, the propagating acoustic waves suffer from several challenges due to the presence of path loss, multi-path propagation, the slow and variant propagation speed, background noise, and Doppler distortion. Since the power supply of the AUVs is limited, communication must be very energy efficient and energy constraints have to be known to be able to plan the mission of AUVs. Due to the difficulties of real experiments, the modeling and simulation of the energy consumption and underwater acoustic communication play an essential role in studying and developing these systems. We provide a modular simulation model for the energy consumption and acoustic underwater communication of AUVs implemented in the network simulator OMNeT++ using the INET framework. More specifically, we extend several INET modules in such a way as to reflect the characteristics of AUVs and underwater communication. We study and analyze the AUVs' energy consumption and dependence of the message quality on different properties such as those mentioned above.

**Keywords** Autonomous underwater vehicles · Energy consumption · Underwater communication · Simulation model

---

✉ Peter Danielis  
peter.danielis@uni-rostock.de

Extended author information available on the last page of the article.

## 1 Introduction

Alone in the German territory of the North Sea and Baltic Sea, there are approximately 1.6 million metric tons of unexploded ordnance (UXO), which has been disposed mostly after World War II (Krawczyk et al. 2018). Even after more than 70 years, the containing partly toxic substances are still reactive. This results in a variety of adverse effects affecting, e.g., the environment, construction project of offshore cable routes and pipelines, port and infrastructure measures, maritime traffic, the fishing industry, and tourism. Recent efforts to deal with this threat focused on the cadastral registration of such objects north.io GmbH (2021), but for large extent its exact location as well as its condition remains unknown. This is mainly due to the sheer amount of these objects as well as the challenging detectability.

There are different technologies for detection and identification of such UXO, mainly via sensor equipment connected to ships or remotely operated vehicles (ROVs) as well as by employment of divers. These solutions, however, are limited by accuracy, costs, and/or safety issues (Bostater Jr 2005). Autonomous underwater vehicles (AUVs) provide a solution to bypass these limitations, especially if applied in collaborative form. Advanced versions of such AUVs are equipped with a survey head comprising multiple sensors and communication modules and are able to operate autonomously over relatively long periods (Atlas Elektronik 2021). Below water, acoustic waves suffer considerably less attenuation compared to radio-frequency signals, turning acoustic communication into the preferred technique for underwater communication (van Walree 2013). Such communication is a fundamental requirement for collaborative AUV operations. However, due to limitations of the energy supply, communication between AUVs as well as the control station must be highly energy efficient. This is especially important, as the energy costs of underwater communication can be comparable to energy costs for underwater movement, e.g., above 60 W just for the acoustic modem (EvoLogics 2020).

In this paper, we present a simulation model for the energy consumption and underwater communication of AUVs implemented in the simulator Objective Modular Network Testbed in C++ (OMNeT++) using the framework Internet networking (INET) (Varga 2010). We extend several INET modules to reflect the characteristics of AUVs and of underwater environments. We use our model to study the energy consumption of AUVs and communication quality between AUVs under water in different scenarios.

The remainder of this paper is organized as follows: In Section 2, we compare our approach with the related work. We introduce the simulation model design and its OMNeT++ implementation in Section 3. In Section 4, we outline the simulation setup and we present results from our OMNeT++ simulations. Finally, we conclude the paper in Section 5, and present directions for future work.

## 2 Related work

This chapter gives an understanding to and summarizes a number of related works for energy models, acoustic underwater communication models, and

simulators, which cover different aspects of energy consumption and the communication channel.

## 2.1 Energy models

This section discusses general models that consider energy consumption. The authors of Stier (2018) describe types of bookkeeping models in particular on software level. In such a model, each operation or each type of instruction is assigned an energy consumption value. Coarser and finer subdivisions into software sections are possible in order to determine more precisely which software operations consume how much energy. This means that energy limitations can be taken into account early in the development process in order to prevent relapses later. Energy models that work with system metrics estimate the power consumption at a given point in time. They do not neglect individual instructions, but rather consider the hardware activity and quantify it using the metrics in order to estimate the energy consumption. The focus of these metrics is, e.g., the power consumption of a processor core or that of a power cable (Stier 2018). Power state machines are a widely applied approach for energy modeling. Here, the energy consumption of a hardware component is modeled by a finite automaton (Stier 2018). In doing so, energy, which is dependent on the current state, is consumed constantly. State transitions can be time or event-related, or as in work (Goraczko et al. 2008) depending on the applied voltage. States can have meaningful names, for example IDLE and STANDBY. Furthermore, status names can contain important parameters, for example the power and frequency currently consumed (Goraczko et al. 2008).

In the following, some recent works are briefly presented that have considered the aspect of energy consumption of AUVs. In Yang et al. (2018), a system was developed that is able to control the hardware of the AUV and, based on mathematical calculations, optimizes the energy consumption of the hardware components depending on the situation in which the AUV is. The movement components of the AUV, i.e., the thrusters, are particularly in focus. Different techniques and models are tested and their performance compared with one another. In contrast to other approaches, only the quality of the controller is examined. However, this model is not able to provide information on the AUV energy consumption over the entire mission time. The authors of Xu et al. (2020) examine long-range AUVs (LRAUVs), a new type of underwater vehicle. The energy available during a mission is the most limiting factor in classic AUVs. Autonomous underwater gliders (AUGs) already partially solve this problem, but their mobility is limited. LRAUVs are a hybrid of AUV and AUG. One can switch their state from AUV to AUG and back. In the referenced work, LRAUVs are analyzed on the basis of efficiency and energy consumption and state of the art technology is described. Energy models are made for many hardware components, the estimated values of which are compared with real measured values. The energy models calculate the energy consumption using mathematical calculation formulas that are as realistic as possible. For the development of these formulas, some values are estimated as constant and other variables are estimated, which will be described in more detail in the work. The focus of this is the development of a mechanism that

improves control during the vertical movement of the LRAUV, which in turn would save energy.

However, current works put little emphasis on the modeling of energy consumption of AUV operations. This is especially true for consumption estimation in case of developments for collaborative operation modes. Hence, we propose in here an energy model, which can be applied for developing advanced strategies for communication-based collaborative operation of AUVs.

## 2.2 Communication models

Xie et al. present Aqua-Sim, a simulator based on NS-2 for underwater sensor networks (Xie et al. 2009). The applied model simulates the attenuation of the acoustic signals and the packet collisions that occur in the network. The authors discuss an attenuation model, which depends on communication distance, frequency, and spreading factor. Due to the challenging conditions in underwater communication, a collision model has been developed for every node. Moreover, four Media Access Control (MAC) protocols have been implemented. Barbeau et al. modeled the physical, link, and network layers of the underwater acoustic communication as well as the mobility of the nodes due to the influence of the communication distance on the communication channel (Barbeau et al. 2015). The model implemented the attenuation, which depends on frequency and communication distance according to the Throp model (Sehgal et al. 2009). The mobility of the nodes presented a variable communication distance, which was used in the attenuation calculations. Finally, the physical layer model has been integrated into OMNeT++. Geng and Zielinski address the limitation of the Rayleigh fading model, which is used in terrestrial communication and commonly used in underwater acoustic communication as well (Geng and Zielinski 1995). They modeled the multi-paths (eigenpaths) and their scattered components (sub-eigenpath components) using a Rice fading model and conclude that the Rayleigh fading model is a particular case of the Rice fading model at small signal-to-multipath ratios. The authors propose an underwater acoustic communication channel simulator that takes into account the several multipaths and their components. Truhachev et al. present a model for a single-input multiple-output underwater acoustic channel (Truhachev et al. 2018). The model considers the multi-path propagation, Doppler distortion, and its effects on frequency and time, as well as the collision of signals at the receiver and their implications on the received signal. Using communication algorithms and experimentally or pre-computed parameters, the authors provide a communication channel that has the same challenges as in the real underwater environment. The model's inputs are power-delay profile, Doppler spread profiles, and some parameters as sampling time. Then based on these inputs, the time variation for each channel tap was modeled, and the transmit/receive filter coefficients were computed. Borowski and Duchamp propose a physical-layer simulation of an underwater channel (Borowski and Duchamp 2010). The simulation is based on measurements that were taken from the underwater environment, such as impulse response, conductivity, temperature, depth, noise, and transmission loss, enabling imitation of the channel distortion and its implications on the signal. The application and link layers of the simulator were developed

using OMNeT++, whereas the physical layer, including signal processing (modulation, convolution, and demodulation), was implemented using MATLAB. Obtained simulation results indicate that the simulator is efficient when the symbol duration is larger than the multi-path spread, and there was no intersymbol interference, and the symbol duration was approximately equal to the delay spread. In addition, the simulator is efficient at using Frequency-Shift Keying (FSK) and Phase-Shift Keying (PSK) modulations at different carrier frequencies. However, the accuracy declined when the symbol time did not exceed the channel's delay spread. Shin and Park present a data transmission simulator that is able to analyze different factors in the underwater environment based (Shin and Park 2008). The propagation speed model is based on Mackenzie's equation which depends on the depth, temperature, and salinity. The model deals with the communication range and depth variation. The transmission loss model depends on spreading, scattering, and absorption, and the noise model consists of ambient noise and momentary noise. The ocean was assumed to be uniform and without refraction or attenuation. Shahabudeen and Chitre conducted simulations using OMNeT++ on different protocols of the physical and data-link layer (Shahabudeen and Chitre 2005). The proposed channel model accounts to compute the propagation delay and the path loss. The noise model is considered to be additive white Gaussian noise. Signal collisions are simulated as they do not interrupt the communication, but the collided packets are considered lost. Signal-to-noise ratio (SNR) is computed using the ambient noise power spectral density. Quadrature Phase-Shift Keying (QPSK) modulation is adopted to calculate the bit error rate, and the probability of losing packets depends on their error rates. Using the ray-tracing propagation method, Çinar and Örencik developed an underwater acoustic channel model in the NS-2 network simulator (Çinar and Örencik 2009). Due to the complexity of using empirical formulas for modeling the communication channel, the authors implemented the ray-tracing technique on a software called Dolphin Underwater Acoustic Propagation (UAP) in order to enable the model to eliminate the effects of multi-path, fading, and shadow zones. The transmission loss and propagation delay are computed through the Dolphin software before passing it to NS-2.

In summary, different models for underwater acoustic communication have been developed focusing on specific aspects of the channel such as multi-path fading, Doppler spread, path loss, networking, MAC protocols, and modulation. While some authors employed empirical measurements to build their models, others used theoretical models, like ray-tracing. However, there is a lack of a holistic modular model that covers the full effects of the underwater environment and enables the consideration of aspects as mobility, power consumption, or application layer. Such a model is proposed in this work.

### 3 Model design and implementation

As discussed above, a holistic model enables the combined consideration of different aspects of collaborative AUV operations, and thus provides a solution for exploring related inter-dependencies.

Having in mind the focus on collaborative AUV operations, the simulation model is developed using OMNeT++ and INET models, which emphasize communication modeling (OpenSim Ltd. 2021). More specifically, the OMNeT++ and INET models have been extended, such that the characteristics of AUVs as well as conditions in underwater environments can be considered.

We model an AUV by using an abstract module that extends the basic built-in OMNeT+ class *SimpleModule* by basic building blocks that submodules have in common, and a *self message* to trigger activity in the simulator. The abstract AUV module comprises submodules modeling the energy consumption, the acoustic communication, the sensors for collecting data, and the movement. Please note that both communication, sensor, and movement model use the energy model.

In the remainder of this section, the main components of this model are presented.

### 3.1 Energy model

The AUV's energy consumption is modeled using several *power state machines* (PSMs) each responsible for a specific subsystem of the AUV. Figure 1 gives an overview of the connections of the individual parts. The *MissionModule* makes sure that the AUV follows its mission plan. The mission plan specifies the mission objectives, for example, the AUV's course and speed by defining several way points and the order in which they have to be visited as well as when to use which sensor for scanning which part of the area. From this mission plan, individual commands are derived for the AUV's subsystems in order to carry out their tasks.

If the energy consumption of a specific subsystem has to be considered, i.e., it is not covered by the base load of the AUV, it needs to be both instrumented and associated with a corresponding PSM. Whenever the subsystem changes an operation mode or issues an action, the instrumented code fires an event that forces the PSM to change into a new state, and thus updating the subsystem's instantaneous energy consumption. The *BatteryModule* integrates the the subsystem's power signal over time and sums up the energy consumption of all subsystems. This way, the *BatteryModule* can calculate at any point in time how much of its initial charge has already

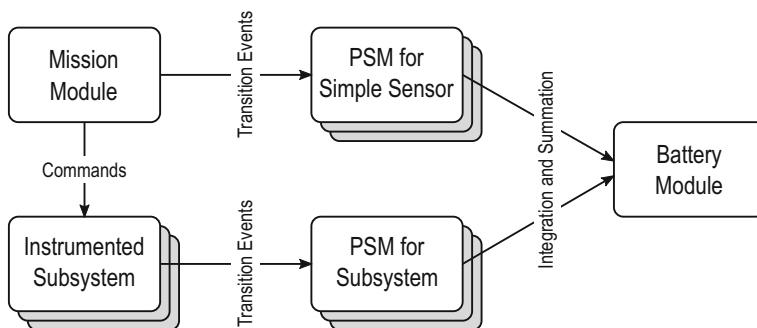


**Fig. 1** Energy model consisting of several PSMs each responsible for an AUV subsystem

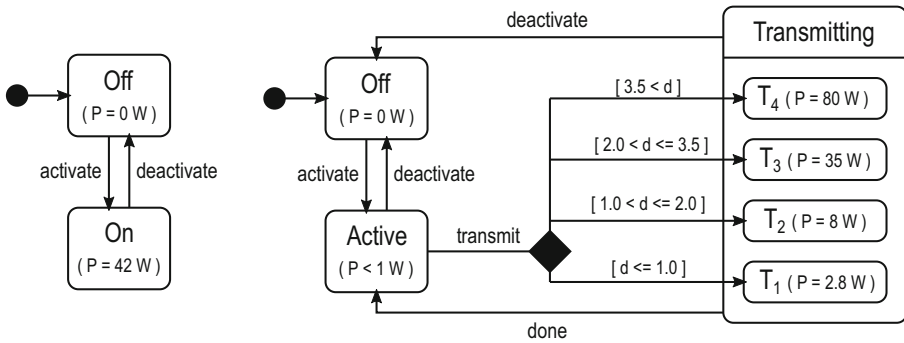


Fig. 2 Left: PSM of a simple sensor. Right: PSM of the acoustic communication modem

been consumed by the AUV and how much energy is still available. Furthermore, a prediction can be made for the remaining maximum mission time.

Please note that it is the simulation’s purpose that primarily determines the required level of detail for modeling the AUV, its subsystems, and their functions. For example, a sub-bottom profiler is a sophisticated acoustic sensor that can produce high-resolution, cross-section images of the sediments below the sea floor. As the gathered data, however, is usually analyzed post-mortem, it has no further influence on the AUVs behavior during its mission. Thus, its simulation role boils down to be an electric consumer that can simply be switched on and off. For convenience, we allow PSMs for those kind of sensors and subsystems to be directly associated with the *MissionModule* from which transition events are then received instead.

Figure 2 (left) shows the PSM for a simple electrical consumer. It has two states representing the device being off and on. Initially, the PSM starts in the *Off* state and it can switch between the *Off* and *On* states by receiving activation and deactivation events, respectively. When being on, the device has a certain power demand (e.g., 42W). The PSM of the AUV’s acoustic communication modem is depicted in Fig. 2 (right). The modem requires the more transmission power the bigger the communication distance grows. This has been modeled by a nested *Transmitting* state that contains several substates with the recommended transmission power setting for a given distance  $d$  in kilometers. Nevertheless, the modem’s PSM is still simplified when compared to its operational model. For instance, the *Active* state subsumes the modem’s standby, listen, and receive modes that all consume less than 1W. For these modes, a more detailed distinction is neglectable when compared to the much larger power demands of other subsystems such as thrusters or imaging sensors or when transmitting data.

### 3.2 Communication model

Figure 3 depicts the acoustic underwater communication channel model. It comprises the physical layer incorporating the radio model for modeling the sending and receiving of data and uses pre-existent INET modules as the application, data link, or network layers to form a complete network stack that allows testing the operation

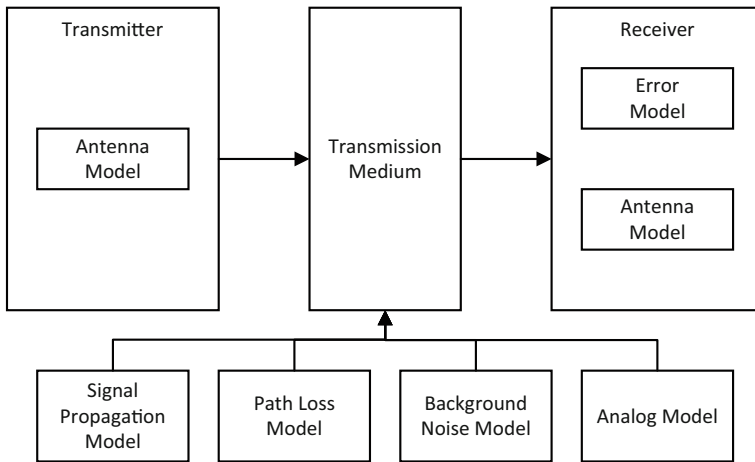


Fig. 3 Block diagram of the acoustic underwater communication channel

of the model. Furthermore, we model the radio medium, which is shared between the different nodes in the communication network, since it is crucial because of its effects on the propagating signals between the network nodes.

### 3.2.1 Radio model

The radio model contains underwater nodes extending the *WirelessHost* module, which represents a network node in INET. A node comprises the underwater radio module responsible for modeling its physical layer. The radio module extends the INET *ApskScalarRadio* module which is able to use different modulation techniques. It describes the physical device that is capable of transmitting and receiving signals on the medium. It is used in conjunction with the scalar radio medium module. The scalar representation is used because the communication is a narrow-band communication.

More specifically, the radio model comprises submodules for transmitter, receiver, error model, and antenna, cf. Fig. 3. The transmitter module extends the INET *ApskScalarTransmitter* module and represents the sending functionality of the acoustic modem of the AUV. The receiver module extends the INET *ApskScalarReceiver* module. It represents the receiver of the acoustic modem, which converts the received acoustic waves into digital data. It computes the signal-to-noise and interference ratio (SNIR) over the transmission duration from the radio medium model. The reception state is determined based on the sensitivity, SNIR threshold, and energy detection parameters. The success of reception depends on the reception power, bandwidth, and modulation as well as on the error model, which is part of the receiver model. The used error model, integrated in the module *ApskErrorModel*, determines the packet error rate, bit error rate, and symbol error rate depending on the formulas that correspond to the used modulation. It is used to model how the signal-to-noise ratio (SNR) affects the errors of the received signals. It expects that no forward error correction



is used in the physical layer. In the model, the error rate is computed for packets by choosing the corruption mode. Furthermore, the acoustic modem's antenna is supposed to have a horizontally omnidirectional radiation pattern. This is a common pattern for the communication in reverberant shallow waters and between horizontal moving or stationary nodes. To model this antenna pattern in 3D, the module *InterpolatingAntenna* is used. The gains of the heading, banks, and elevation planes of the Euler angles are specified independently of each other as a sequence of angle (degree) and gain (dB) pairs for each plane. The antenna is placed on the top center of the AUV. Because of its directive radiation pattern and its location, the transmitted signals will not reach the receiver if it is located beneath the transmitter.

### 3.2.2 Radio medium model

The radio medium model contains the radio medium module, which represents the shared physical medium, where the communication takes place. This module keeps track of transceivers, sources, ongoing transmissions, and noise. It extends the INET *ApskScalarRadioMedium* module. More precisely, the radio medium module provides submodules for modeling the signal propagation, background noise, path loss, and the analog representation of signals, cf. Fig. 3. The propagation of the acoustic signals underwater is one of the most distinct factors that influence the performance of the communication system. It is characterized to be slow and variant depending on the temperature, pressure, and salinity, which all change with the depth. Its values change from 1490 to 1510 m/s. This has implications on the transmitted signal, such as the high delay, the multi-path fading, and the Doppler distortion, which can reduce the system's throughput considerably. The signal-propagation module extends the INET *ConstantSpeedPropagation* module. The propagation speed is chosen to be 1500 m/s, which is the average speed. For missions operated in specific depths, the propagation speed does not change much. The background-noise module is used to describe the total noise that affects the communication channel. This noise model does not change with space, time, and frequency. It provides noise used in scalar computations at the receiver to decide if the packets are received successfully. The error model of the receiver uses the background noise to compute the error of the received signals. The used bandwidth of the noise signal is 16 kHz. The path-loss model compares the performance of the Rayleigh fading and the Rician fading models. The Rayleigh fading describes the channel when there is no dominant component present in the received multi-path signals. The propagating signal power is randomly decreased according to a Rayleigh distribution. The Rician model considers that the channel is not a fully scattering channel, but the channel may have several distinct signal paths or dominant signals (Geng and Zielinski 1995). The Rician fading K-factor is the ratio of the signal power of the dominant path over the signal power of the scattered paths. When the K-factor is equal to zero, the channel is Rayleigh, but if it is equal to infinite, the channel is Gaussian (Chaitanya et al. 2011). Both models are adopted to describe the path loss in the acoustic underwater communication channel (Socheleau et al. 2009; Park et al. 2010; Yang and Yang 2006; Christhu Raj and Sukumaran 2016). Based on the INET *ScalarAnalogModel* module, an analog model is developed that combines the effects of the antenna and path loss modules

**Table 1** Selected common sensors of an AUV

| Sensor name          | Functionality       | Data type          |
|----------------------|---------------------|--------------------|
| Doppler velocity log | Data collection     | Environmental data |
| Camera               | Image acquisition   | Images             |
| Multi-beam           | Data collection     | Environmental data |
| Side scan sonar log  | Data collection     | Environmental data |
| Sub bottom profiler  | Data collection     | Environmental data |
| Surround sonar       | Collision avoidance | Environmental data |

and computes the received signal from the transmitted signal. Since the scalar representation is used for the transmitter, receiver, and transmission medium, the scalar analog model is used.

### 3.3 Sensor model

The main motivation for using an AUV is the automated and autonomous collection of data from marine areas. The built-in sensors are therefore one of the most important aspects when simulating an AUV. Table 1 lists a typical selection of sensor of an advanced AUV. The camera is used to collect images; the surround sonar to avoid collisions with unexpected objects. The remaining sensors enable the collection of data, e.g., for terrain models and similar.

The sensor model, which contains the common elements of all sensors, includes the energy model and is derived from the abstract AUV model. This includes, among other elements, a common mode of operation. When the mobility controller detects a discrete change in position, each sensor is notified of the change that has occurred. In conjunction with a defined sampling rate, the sensor is then able to collect information about an environment that has yet to be implemented, and store it in a storage module. This data can then be stored in a specific memory of the AUV. Please note that the sensor model is still under construction. As part of our future work, we will extend it to make it more realistic and evaluate the impact of sensor measurements on the AUV movement (e.g., in case an obstacle is detected) as well as the influence of sensor activity on the energy consumption.

### 3.4 Movement model

As part of our ongoing work, a movement logic provided by built-in INET models was implemented without considering physical laws (INET Core Team 2021). The main focus is the ability to test other components that rely on movement data. For instance, the energy consumption during movements is influenced by the way in which the thrusters (such as bow and vertical thrusters) are used (cf. Section 3.1). Prospectively, a more realistic movement model will be designed that considers the effects of forces in underwater environments.

## 4 Evaluation

Different scenarios are simulated in OMNeT++ to evaluate the developed models and the overall functionality of the proposed approach.

### 4.1 Evaluation of the energy model

To evaluate our energy models, we devised and simulated several missions for a single AUV with different usage profiles for thrusters, communication modem, and sensors. In the *light* usage profile, the AUV continuously moves slowly and only sends periodic position updates over very short distances to the base station, whereas in the *heavy* usage profile, both thrusters and communication modem operate at full power over the full mission time. In both cases, all carried sensors (c.f. Table 1) stay active throughout the mission. In contrast, the *mixed* usage profile comprises distinct intervals with slow and fast movement, and with and without data communication at different distances as well as a short period with most of the sensors being shut off. This usage pattern is repeated every 60 min.

The simulation results are shown in Fig. 4. The left diagram graphs the instantaneous power consumption of the AUV for the first 3 h of the mission, whereas the right diagram shows the AUV's decreasing battery level over the whole mission time. In fact, we continued the simulation until the battery was completely depleted in order to determine the maximum mission time possible for the given usage profile. Here, with about 8h 45min the heavy profile and with approximately 12h 30min the light profile define a lower and an upper bound, respectively, of a time window for a meaningful mission. Since the AUV's power demand remains constant in both profiles, these values can also be calculated manually without much effort. However, for dynamic usage patterns such as the mixed profile (cf. Fig. 4 (left)), this becomes less practical. Hence, with AUVs performing increasingly independent, complex, and dynamic missions, the advantages of a simulation pay off. In our case, the simulation of the mixed profile resulted in a maximum mission time of about 11h 10min (cf. Fig. 4 (right)).

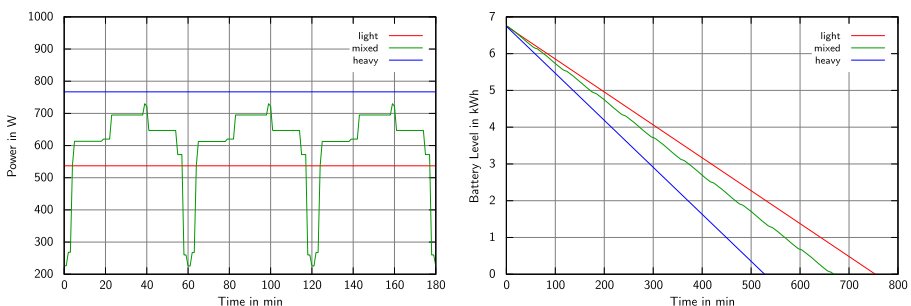


**Fig. 4** Left: Instantaneous power consumption for different mission profiles. Right: Battery level for different mission profiles

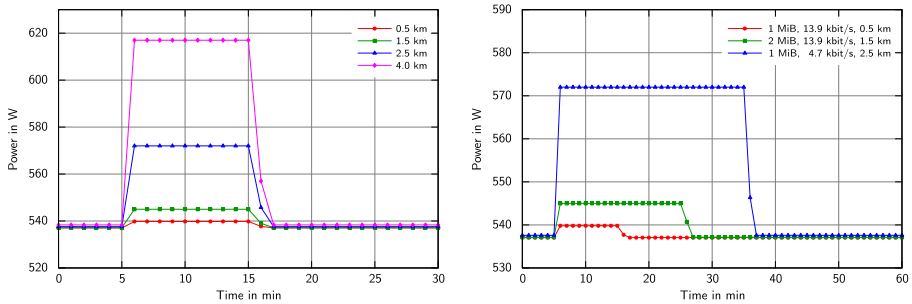


**Fig. 5** Left: Power demand for different communication distances. Right: Power demand for different data sizes and data rates

Besides simulating the energy budget of the whole AUV, it is also possible to analyze the energy consumption of its subsystems and their respective dependencies. Figure 5 presents the simulation results for the acoustic communication modem that starts sending a message 5 min after the beginning of the simulation. The left diagram clearly shows that the power demand for transmitting the message depends on the communication distance. In fact, this directly reflects the dependency explicitly modeled by the modem's power state machine (PSM) in Section 3.1. Furthermore, the modem's energy consumption indirectly depends on the size of the message to be sent and the modem's data rate as can be seen in the right diagram. This is because the transmission time grows proportionally with the message size, whereas it decreases inversely proportionally with the data rate. Please note that different communication distances have been chosen for the sake of clarity only. Otherwise, the curves overlap and partially obliterate each other.

## 4.2 Evaluation of the communication model

Various parameters of the transmission medium, transmitter, and receiver are compared to study the influences of these parameters on the quality of the communication. This communication quality is represented via the number of successfully received packets over the transmission range. The successful reception of a packet means that the signal that reached the receiver has the minimum acceptable reception power and error rate as well as the bandwidth, modulation, and synchronization between the transmitter and receiver.

### 4.2.1 Simulation setup

The simulation scenario consists of two AUVs: NodeA and NodeB; see Fig. 6 for a 3D visualization in OMNeT++. NodeA sends a UDP packet every 2 s to NodeB. The simulation time is set to be 120 s, making NodeA send 60 packets during the whole simulation duration. The default model parameters are shown in Table 2. Note that in each simulation scenario, the respective parameter is tested at different values, and the rest of the parameters are set as the default values.

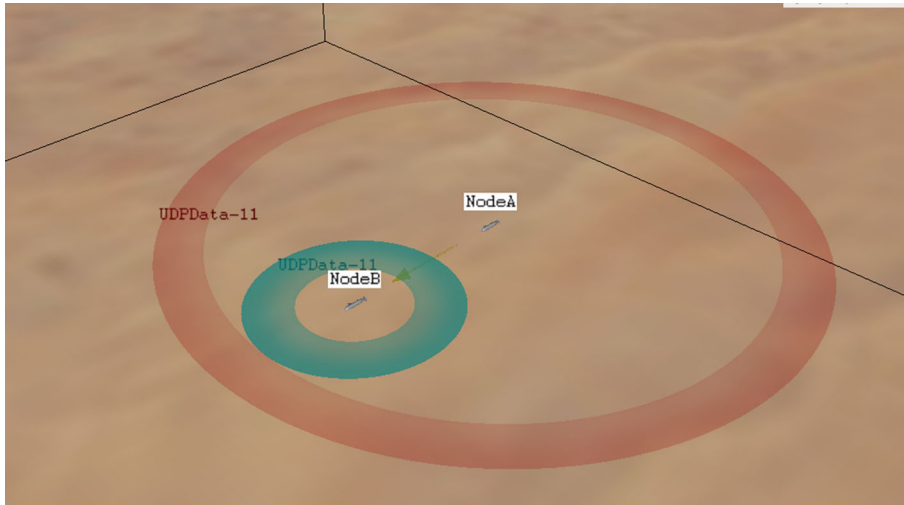


**Fig. 6** 3D visualization of the simulation scenario

#### 4.2.2 Simulation results

The test cases are chosen to highlight the impact of the operating frequency band, background noise power, transmitting power, Rayleigh fading system loss, Rician fading system loss and K factor, receiver sensitivity and SNIR threshold, and antenna directivity on the number of received packets.

**Operating frequency band** To show the dependence of the operating frequency on the transmission range and the system performance, the model is tested at different frequency bands. Figure 7 (left) depicts the obtained results, i.e., the number of

**Table 2** Default simulation parameters

| Parameter                   | Value      |
|-----------------------------|------------|
| Background noise power      | 1 dBm      |
| Transmitting power          | 80 W       |
| Rayleigh fading system loss | 2 dB       |
| Receiver sensitivity        | 2 dBm      |
| Receiver SNIR threshold     | 2 dB       |
| Receiver energy detection   | 1 dBm      |
| Frequency band              | 18–34 kHz  |
| Bitrate                     | 13.9 kbps  |
| Default message length      | 2 B        |
| Preamble duration           | 10 $\mu$ s |
| UDP header length           | 8 B        |

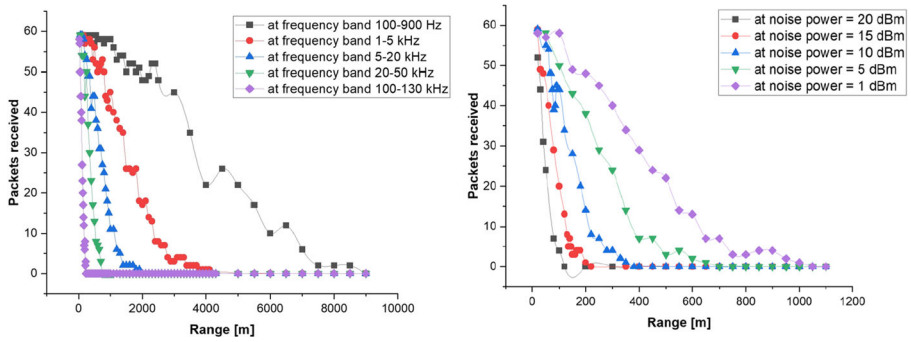


**Fig. 7** Left: Number of received packets over the transmission range at different frequency bands. Right: Number of received packets over the transmission range at background noise power values

received packets over the transmission range at different frequency bands. The values of the frequency band are chosen based on Shin and Park (2008). Furthermore, all parameters of the other modules are set to the default values listed in Table 2.

As apparent from the graph, the transmission range depends notably on the operating frequency band, i.e., lower frequency bands enable longer distances. For frequency band 100–130 kHz, the performance of the communication system drops significantly after approximately 100–200 m. The receiver does not receive any packets after 230 m. In case of the 20–50-kHz band, the possible communication range increases almost three times. The receiver receives half of the sent packets successfully at 350 m and stops receiving any packets after 700 m. At the frequency band 5–20 kHz, almost half of the packets are received at 700 m, and the communication stops after 1900 m. The performance for the 1–5-kHz band is almost double. Communication is not possible after 4100 m. Finally, for 100–900 Hz, the communication range remarkably increases to reach 8500 m for the last possible reception. Furthermore, 85% of the packets are received successfully at 1900 m.

**Background noise** Figure 7 (right) illustrates the impact of the background noise on the performance of the system over the communication range. The noise power values indicate the total noise present in the communication environment and are compared to test different environment scenarios. The bandwidth of the background noise is set to match the operating frequency of the transmitter and the receiver.

As expected, the performance of the system depends on the background noise. When applying higher noise power values, the number of received packets witnesses a considerable decline at the same communication range. At noise power equal to 20 dBm, the receiver does not receive packets for ranges beyond 120 m. Even for very short distances like 20 m, 52 out of 60 packets are received successfully. The performance is roughly doubled for noise power of 15 dBm, at which the maximum possible communication range increases to 220 m. For noise power of 10 dBm, the receiver receives about half of the packets at range 150 m and does not receive any packet after 350 m. In the case of 5-dBm noise power, the communication range increases almost twice compared to the 10 dBm case. The performance improves

significantly when applying the minimum noise power, which equals to 1 dBm. Half of the packets are received successfully at 400 m, while no packets are received after approximately 1000 m.

**Transmitting power** Acoustic modems for underwater communication use different transmitting power options to send messages for different communication ranges.

In here, we assume four different transmitting power options, which have been individually tested. Figure 8 (left) depicts the obtained results, i.e., the number of packets received over the transmission range for each transmitting power option. As expected, using a higher transmitting power considerably increases the communication range. In the case of using 2.8-W transmitting power, the last successful reception of any packets is limited to be about 200 m. In case of 8 W, the maximum communication range improves slightly to 300 m. This figure is doubled when using 35-W transmitting power and results in 700 m for the last reception possible and 250 m to receive successfully half of the packets. When using the maximum transmitting power, 80 W, half of the packets are successfully transmitted until nearly 400 m, while the maximum communication range is 1000 m.

**Comparison between fading models** Next, Rayleigh and Rician fading models, which have been adapted to model the path loss for the underwater acoustic communication, are compared to determine the related impact on the communication quality.

Figure 8 (right) shows the obtained simulation results, i.e., the comparison between both models on the number of packets received versus the communication range. The Rayleigh fading model is configured with a system loss of 2 dB, while the Rician fading model is set with a system loss of 2 dB and a K factor of 4. The results indicate, that for the first 400 m, the system with the Rician fading model has better performance regarding the number of packets received. Beyond that range, both models show a slightly matching performance.

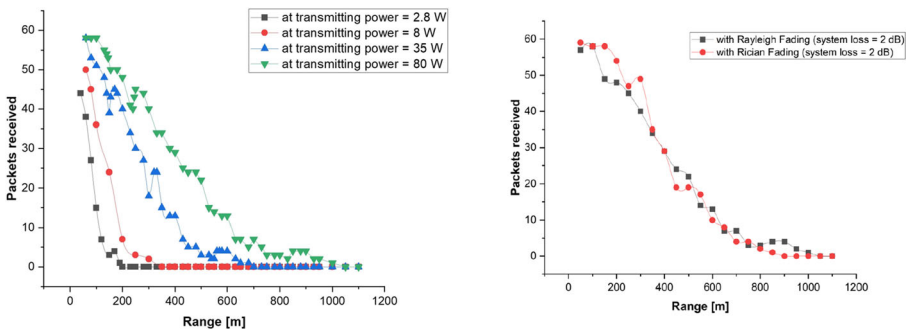


**Fig. 8** Left: Number of packets received over the transmission range using different transmitting power. Right: Comparison between Rayleigh and Rician fading effect models on the number of packets received over the communication range

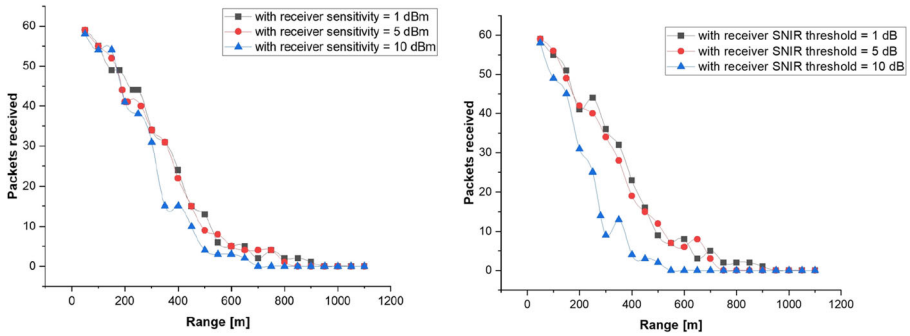


**Fig. 9** Left: Receiver sensitivity effect on the number of received packets over the communication range. Right: Receiver SNIR threshold effect on the number of received packets over the communication range

**Receiver sensitivity and SNIR threshold** The receiver sensitivity determines the minimum signal power at which the receiver detects the incoming signals. As the path loss model reduces the propagating signal power, the receiver sensitivity has important implications on the design of the model.

In Fig. 9 (left), different values of the receiver sensitivity are compared to show how the receiver behaves with the Rayleigh fading model using different receiver sensitivity values. One can notice that when using a receiver sensitivity of 1 dBm and 5 dBm, the number of received packets has slightly the same performance. In case of 10 dBm, the number of received packets is initially similar to the two previous values, but drops notably stronger from 300 m on.

The receiver SNIR threshold determines the minimum acceptable SNIR that the receiver can successfully receive the packets. In Fig. 9 (right), the model is tested with 1-, 5-, and 10-dB SNIR thresholds to find its dependence on the system. The number of received packets over the communication range has slightly the same behavior for the 1- and 5-dB cases. On the other hand, in the case of 10 dB, the number of received packets significantly drops over the range and reaches zero after around 500 m.

**Antenna directive** The antenna used in an acoustic modem usually has a horizontal omnidirectional radiation pattern. Consequently, it does not send or receive messages if the two AUVs are located on top of each other.

To test the antenna directivity, a linear mobility model is used to move NodeB beneath NodeA. During the test, NodeA sends a UDP packet every 2 s, while NodeB sends back every message it receives. Figure 10 shows the timeline of the packet activity between NodeB and NodeA, while NodeB is moved (not shown). At the start of the simulation, both NodeB and NodeA are in the radiation direction region, so messages go back and forth between both (indicated by the blue arrows with labels UDPData-2 and UDPData-3). In the red-shaded time range, NodeB is moved beneath NodeA and no message is sent or received. Afterwards, NodeB reaches again the radiation directivity of NodeA's antenna and messages are exchanged again.



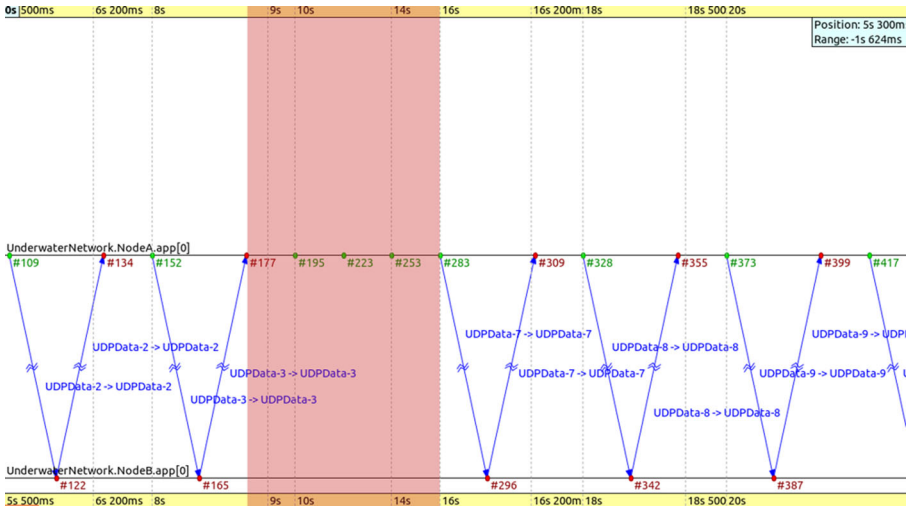


**Fig. 10** Timeline of the sent and received packet activities between NodeA and NodeB during the antenna directivity test. NodeB is moved (not shown) and is located beneath NodeA in the red-shaded time range. The blue arrows indicate messages that have been sent by NodeA and returned by NodeB

## 5 Conclusion

This paper presents a simulation model of AUVs, with emphasis on energy consumption and underwater communication. As proof of concept, the model was implemented in OMNeT++ by extending several INET modules in such a way as to reflect the characteristics of AUVs and underwater environments.

The approach of modeling the energy consumption of AUVs with power state machines has proven to be target-oriented and useful. It turns out that the energy consumption can already be determined very well with theoretical values from handbooks. A better calibration of the model with realistic values is effortlessly possible, since the simulation model can be adapted easily and flexibly. With the help of the simulation results, complex mission runs can be planned, since one can plan the energy consumption of the AUVs and thus the duration of missions.

The obtained results for the communication model indicate the influence of the frequency band, background noise power, transmitting power, fading system loss, receiver sensitivity and SNIR threshold, and antenna directivity on packet loss, which makes underwater very different from terrestrial communication. To summarize our results, as expected, of 60 sent packets, we observe a decreasing number of received packets with increasing background noise power, fading system loss, receiver sensitivity, and receiver’s SNIR threshold while we see an increasing number of received packets for increasing transmission power. Furthermore, lower frequency bands achieve much longer distances. The simulations also show that the antenna works according to its specification allowing for horizontally omnidirectional transfers while considering the antenna’s blind spot under an AUV.

In our ongoing work, we will conduct experiments to verify our findings obtained through simulation as well as we will extend and evaluate further submodules of our model such as a sensor and a movement model.

**Acknowledgements** A previous version of the current paper was presented at MARESEC 2021 with the title "Modeling Underwater Communication for Autonomous Underwater Vehicles in OMNeT++".

**Funding** Open Access funding enabled and organized by Projekt DEAL.

## Declarations

**Conflict of interest** The authors declare no competing interests.

**Open Access** This article is licensed under a Creative Commons Attribution 4.0 International License, which permits use, sharing, adaptation, distribution and reproduction in any medium or format, as long as you give appropriate credit to the original author(s) and the source, provide a link to the Creative Commons licence, and indicate if changes were made. The images or other third party material in this article are included in the article's Creative Commons licence, unless indicated otherwise in a credit line to the material. If material is not included in the article's Creative Commons licence and your intended use is not permitted by statutory regulation or exceeds the permitted use, you will need to obtain permission directly from the copyright holder. To view a copy of this licence, visit <http://creativecommons.org/licenses/by/4.0/>.


## References

- Atlas Elektronik (2021) Seacat product description. <https://www.atlas-elektronik.com/solutions/mine-warfare-systems/seacat.html>
- Barbeau M, Blouin S, Cervera G et al (2015) Simulation of underwater communications with a colored noise approximation and mobility. In: 2015 IEEE 28th Canadian Conference on Electrical and Computer Engineering (CCECE). IEEE, pp 1532–1537
- Borowski B, Duchamp D (2010) Measurement-based underwater acoustic physical layer simulation. In: OCEANS 2010 MTS/IEEE Seattle. IEEE, pp 1–8
- Chaitanya DE, Sridevi CV, Rao GSB (2011) Path loss analysis of underwater communication systems. In: IEEE Technology Students' Symposium. IEEE, pp 65–70
- Christhu Raj M, Sukumaran R (2016) Stochastic network calculus for rician fading in underwater wireless communication networks. *Appl Math Inf Sci* 10(4):1–10
- Çinar T, Örencik MB (2009) An underwater acoustic channel model using ray tracing in ns-2. In: 2009 2nd IFIP Wireless Days (WD). IEEE, pp 1–6
- EvoLogics (2020) Underwater acoustic modems - product information guide
- Geng X, Zielinski A (1995) An eigenpath underwater acoustic communication channel model. In: Challenges of Our Changing Global Environment'. Conference Proceedings. OCEANS'95 MTS/IEEE. IEEE, pp 1189–1196
- Goraczko M, Liu J, Lymberopoulos D et al (2008) Energy-optimal software partitioning in heterogeneous multiprocessor embedded systems. In: 2008 45th ACM/IEEE Design automation conference. IEEE, pp 191–196
- INET Core Team (2021) INET mobility models. <https://inet.omnetpp.org/docs/showcases/mobility/basic/doc/>
- Bostater Jr CR (2005) On reduction of risks in UXO and mine detection using remote sensing systems and related synthetic image simulation. In: Detection and remediation technologies for mines and minelike targets X, vol 5794. SPIE, pp 42–55. <https://doi.org/10.1117/12.607533>
- Krawczyk S, Sass S, Kluge M (2018) Historical investigation and risk mitigation for the identification of unexploded ordnance (uxo) in the north sea and baltic sea. In: 2018 IEEE/OES Baltic International Symposium (BALTIC), pp 1–5. <https://doi.org/10.1109/BALTIC.2018.8634857>

- north.io GmbH (2021) Amucad. <https://amucad.org/>
- OpenSim Ltd. (2021) OMNeT++ Discrete event simulator. <https://omnetpp.org/>
- Park J, Park KC, Yoon JR (2010) Underwater acoustic communication channel simulator for flat fading. *Japanese J Appl Phys* 49(7S):07HG10
- Sehgal A, Tumar I, Schonwalder J (2009) Variability of available capacity due to the effects of depth and temperature in the underwater acoustic communication channel. In: OCEANS 2009-EUROPE. IEEE, pp 1–6
- Shahabudeen S, Chitre MA (2005) Design of networking protocols for shallow water peer-to-peer acoustic networks. In: Europe Oceans 2005. IEEE, pp 628–633
- Shin SY, Park SH (2008) Omnet++ based simulation for underwater environment. In: 2008 IEEE/IFIP International Conference on Embedded and Ubiquitous Computing. IEEE, pp 689–694
- Socheleau FX, Passerieux JM, Laot C (2009) Characterisation of time-varying underwater acoustic communication channel with application to channel capacity. In: Underwater acoustic measurements
- Stier C (2018) Adaptation-aware architecture modeling and analysis of energy efficiency for software systems. PhD thesis, Karlsruhe Institute of Technology, Germany
- Truhachev D, Schlegel C, Bashir M et al (2018) Modeling of underwater acoustic channels for communication system testing. In: OCEANS 2018 MTS/IEEE Charleston. IEEE, pp 1–8
- Varga A (2010) OMNeT++. Springer, Berlin Heidelberg, pp 35–59. [https://doi.org/10.1007/978-3-642-12331-3\\_3](https://doi.org/10.1007/978-3-642-12331-3_3)
- van Walree PA (2013) Propagation and scattering effects in underwater acoustic communication channels. *IEEE J. Ocean. Eng.* 38(4):614–631. <https://doi.org/10.1109/JOE.2013.2278913>
- Xie P, Zhou Z, Peng Z et al (2009) Aqua-sim: An ns-2 based simulator for underwater sensor networks. In: OCEANS 2009. IEEE, pp 1–7
- Xu H, Zhang GC, Sun YS et al (2020) Energy-saving control of long-range autonomous underwater vehicle vertical plane based on human simulating intelligent control method. *Int J Adv Robot Sys* 17(5):1729881420944,744
- Yang N, Amini MR, Johnson-Roberson M et al (2018) Real-time model predictive control for energy management in autonomous underwater vehicle. In: 2018 IEEE Conference on Decision and Control (CDC). IEEE, pp 4321–4326
- Yang WB, Yang T (2006) Characterization and modeling of underwater acoustic communications channels for frequency-shift-keying signals. In: OCEANS 2006. IEEE, pp 1–6

**Publisher's note** Springer Nature remains neutral with regard to jurisdictional claims in published maps and institutional affiliations.

## Affiliations

Peter Danielis<sup>1</sup>  · Helge Parzyjgla<sup>1</sup> · Mostafa Assem Mohamed Ali<sup>1</sup> · Frank Sill Torres<sup>2</sup>

Helge Parzyjgla  
helge.parzyjgla@uni-rostock.de

Mostafa Assem Mohamed Ali  
mostafa.ali@uni-rostock.de

Frank Sill Torres  
frank.silltorres@dlr.de

<sup>1</sup> Institute of Computer Science, University of Rostock, Albert-Einstein-Straße 22, Rostock, 18059, Mecklenburg-Vorpommern, Germany

<sup>2</sup> Resilience of Maritime Systems, German Aerospace Center (DLR), Fischkai 1, Bremerhaven, 27572, Bremen, Germany